Archaeological and Anthropological Sciences (2021) 13: 135
https://doi.org/10.1007/s12520-021-01414-0

ORIGINAL PAPER

The implication of technology and chronology reflected in a group of iron objects from the archeological site at Talgar in southeast Kazakhstan

Jang Sik Park[1] · **Tamara Savelieva**[2]

Received: 7 March 2021 / Accepted: 4 July 2021 / Published online: 15 July 2021

Abstract
Talgar in southeast Kazakhstan was one of the flourishing medieval towns in Central Asia that faced the Mongol invasion, which led to little textual or material evidence documented of subsequent human residence. A metal assemblage consisting of eight iron tools and a lighting device recently excavated from what is typically considered a medieval site at Talgar shed new light on Talgar's post-medieval history. Metallographic and radiocarbon examination showed that these objects were manufactured during the mid-fifteenth to the early seventeenth century AD period under a technological environment based on the production of bloomery iron and the implementation of carburization and quenching techniques. This particular iron-working tradition could not be established without the full understanding of material properties as determined by carbon concentration and thermomechanical treatments. This article characterizes the technology and chronology of the given iron objects. The outcome is then placed in comparative perspective to probe plausible continuity in technological traditions between the pre- and post-Mongol communities of the region.

Keywords Talgar in Kazakhstan · Medieval site · Post-Mongol period · Iron technology · Radiocarbon

Introduction

Recent studies on the iron assemblages from the medieval sites at Talgar (Park and Voyakin 2013) and Kastek (Park and Arnabai forthcoming) in southeast Kazakhstan (Fig. 1) have documented a virtually identical technological tradition based primarily on bloomery iron with cast iron being used as a supplement. The periodization based on typological estimation and radiocarbon measurements placed the assemblages from Talgar and Kastek mostly within the range of the tenth to thirteenth century AD and the seventh to thirteenth century AD, respectively. It is important to note that similar bloomery-based technology had long been in practice as a major iron-making method in Mongolia from the Xiongnu (3rd BC to second century AD) to the Mongol period (13th to fifteenth century AD, Park et al. 2010; Park and Reichert 2015). Bloomery-based technology widely practiced in these regions, however, stands in strong contrast to cast iron-based technology, which was established as the dominant iron-making tradition in China from the Han dynasty (206 BC-220 AD) onward. Iron smelting in bloomery furnaces was also practiced in China but only as an alternative where cast iron-based iron production was deemed impractical (Larreina-Garcia et al. 2018).

Given iron production being one of the major aspects of material culture and China's key role in the region's sociopolitical and cultural landscape, the above observation suggests that geographic proximity was not necessarily a defining factor for the transmission and adoption of technological ideas and practices. The distinct bloomery-based iron tradition, supplemented by the use of cast iron, was likely related to Central Asia's unique role diffusing diverse technologies practiced in various parts of the Eurasian continent. The evolution of local iron technology, when studied in a wider comparative perspective, may then serve as a means for understanding Central Asian communities' interactions

✉ Jang Sik Park
jskpark@hongik.ac.kr

Tamara Savelieva
tsavelieva@mail.ru

[1] Department of Materials Science and Engineering, Hongik University, Sejongro Jochiwon, Sejong 30016, South Korea

[2] Margulan Institute of Archaeology, 44, Dostyk Ave, 480100 Almaty, Republic of Kazakhstan

Fig. 1 Map of the Republic of Kazakhstan. **a** Kazakhstan and the neighboring countries; **b** a map enlarging the rectangular area indicated in Fig. 1a. Arrow 1 locates the medieval site at Talgar, from which the objects under investigation were excavated. Arrow 2 indicates the medieval site at Kastek

with their neighbors and their impact on the region's cultural development. This approach takes on new significance with the recent excavation of an iron assemblage that dates back to the post-medieval period after the Mongol invasion of the thirteenth century, despite having been discovered from within the medieval site at Talgar (Fig. 1a and b). Most artifacts thus far excavated at the Talgar site came from pre-Mongol contexts and little evidence, whether textual or archeological, is currently available for notable cultural activities during the subsequent period.

We examined the objects for microstructure, chemical composition, and radiocarbon age to define the pertinent technological tradition, which were then compared with that of objects previously excavated from the same site, dated as being from a period before the Mongol invasion. We present the detailed account of the results to confirm the occupation of the site during the post-Mongol period and also to address the issue of technological continuity or discontinuity between the former and latter iron-making traditions.

Comments on site and artifacts

Situated approximately 25 km to the east of Almaty (Fig. 1b) in the southeastern part of Kazakhstan, called Semirechye, the site at Talgar has been a major settlement for centuries. The region of Semirechye is bounded by the Zailiisky Alatau Mountains to the South, the Dzunghar Alatau Mountains to the Northeast, and the Balkhash Desert to the West. Located at the crossroads between the desert-oasis region of Central Asia proper and the semi-arid and desert areas of Mongolia and western China, Semirechye played an important role in the establishment and operation of a branch of the Great Silk Road from around BC 130 through the fourteenth to fifteenth century AD (Frachetti 2008). Medieval Talgar was one of the steppe towns and cities that had developed along this Silk Road in Semirechye from the eighth century AD and flourished until it faced the Mongol invasion at the beginning of the thirteenth century AD (Chang et al. 2002: 44).

The settlement was apparently established at the time the Islamic force was invading Central Asia while the Chinese Tang dynasty was constantly vying for hegemony over the region. The site must have seen the fall of the Turkic confederacy, which led to the fragmentation of the state into its constituent tribal groups. The decline of Chinese influence following its defeat against the Islamic army at Taraz (Fig. 1a) in the year 751 placed the region under the control of the Karluk, a Turkic tribe, which played a key role in the Islamic army's victory at Taraz. Subsequently, the Karluk secured support from other Turkic tribes to establish the Karakhanid Khaganate, the first major Islamic state of Turkic origin in Central Asia, with its capital located at Balasagun near the modern city of Tokmok (Fig. 1b) in Kyrgyzstan, approximately 167 km to the southwest of Talgar (Frye 2004).

The medieval site at Talgar has long been under excavation headed by Tamara Savelieva of the Margulan Institute of Archaeology, leading to the recovery of numerous iron objects along with a variety of other cultural remains (Chang et al. 2002; Park and Voyakin 2009, 2013). The iron objects under investigation, recently recovered within the site, were all placed together in an enclosed space as if to avoid being stolen or plundered.

The external appearance of the objects is illustrated in Fig. 2 where all the artifacts are shown approximately to scale, each with a number for identification and the arrows indicating the places where samples were taken for examination. Visual inspection of Fig. 2 makes it clear that objects #1 through 8 were forged to shape while #9, a lamp accessory, was shaped by casting. Those made by forging consist of a plow (#1), a pick (#2), two axes with a hole for hafting (#3 and 4), two axes without such a hole (#5 and 6), and two adzes with an empty space prepared apparently for inserting a handle (#7 and 8). It should be noted that objects #3 and 4 have an asymmetric blade with one side taking a more prominent shape than the other side.

Radiocarbon measurement

Object #9 in Fig. 2, a cast iron lamp accessory, was radiocarbon dated using accelerator mass spectrometry (AMS). A metal piece of approximately 1 g was taken from the object and sent for radiocarbon measurement at the Centre for Applied Isotope Studies of the University of Georgia (UGAMS) in the USA, where a carbon sample was extracted from it.

The radiocarbon data are summarized in Table 1, where the 1σ ^{14}C age was calculated from the values obtained in the measurement of ^{14}C concentrations (Donahue et al. 1990). The calendar date was then computed using OxCal v.4.4 (Bronk Ramsey 2009) in conjunction with the extended ^{14}C database IntCal20 (Reimer et al. 2020) and graphically illustrated in Table 1. The 1σ **^{14}C** age was determined at 360 ± 20 years before present (yr BP) as of 1950, which, when calibrated, gives the calendar date within 2σ-probability range (95.4%) of 1459–1632 AD. This result indicates that the object in question was cast to shape using cast iron that was smelted sometime between the mid-fifteenth and the early seventeenth century AD in a charcoal-fired operation.

The radiocarbon result above serves to confirm the presence of substantial human activities in the region during the period determined, which is rarely observed in documentary or material evidence currently available. Given that mineral coal-fired smelting was dominating the contemporary

Fig. 2 The general appearance of the iron objects examined. The artifacts are shown approximately to scale, each with a number for identification. The arrows indicate where samples were taken for examination. Object #1 is a plow, #2 a pick, #3 and 4 axes with a hole for hafting, #5 and 6 plate-type axes, #7 and 8 adzes with a space prepared apparently for inserting a handle, and #9 a cast iron lamp accessary. Objects #1–8 were all forged to shape while #9 was cast into shape

Table 1 Result of the AMS radiocarbon measurement on a carbon sample extracted from object #9 in Fig. 2, a lighting device made of cast iron, recovered from the medieval site at Talgar, Kazakhstan. The measurement was made in the University of Georgia's Centre for Applied Isotope Studies (CAIS)

Lab Code	$\delta^{13}C$ (‰)	1σ ^{14}C age (yr BP)	95.4% (2σ) Cal. age ranges (AD)	Comments
UGA30809	-23.71	360±20	1459-1632	Sample ID TG-9

Graphical illustration of the calibrated calendar date

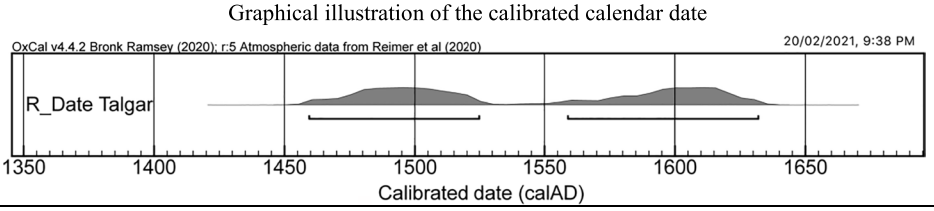

cast iron industry of Mongolia (Park et al. 2008, 2019; Park 2015), likely reflecting the charcoal-to-mineral coal transition in China (Wagner 2008: 311–320), evidence of a charcoal-fired process in practice could point to another important possibility that a small-scale production of cast iron was locally implemented.

Microstructure examination

For metallographic examination, specimens were taken from each of the objects in Fig. 2 at the locations marked by the arrows. The specimens were mounted and polished following standard metallographic procedures and then etched using a solution of 2% nitric acid by volume in methanol. They were examined for microstructural characteristics using an optical microscope and a scanning electron microscope (SEM). The microstructural data were used to infer carbon concentrations and the nature of thermal treatments applied. The presence of other minor elements was checked using the energy dispersive x-ray spectrometer (EDS) included with the SEM, whose detection limit is approximately a few tenths of a percent. The microhardness of the specimens was measured with a Vickers diamond pyramid indenter using a load of 500 g and specified in Vickers hardness number (VHN).

The specimens taken at arrows a and b of object #1 of Fig. 2, a plow, displayed a similar microstructure consisting primarily of ferrite grains, the carbon content of which is 0.02% or less. A little pearlite was observed near the surface of the specimen from arrow a, suggesting that the pointed end had been carburized to form a high carbon surface layer, which was almost worn out with use.

The specimens from arrows a and b of object #2, a pick, were almost identical in their microstructures, as illustrated in Fig. 3a, an optical micrograph showing the structure at arrow b. Figure 3a is seen to consist of the ferrite phase divided into numerous small areas in the form of rods or needles, with their boundaries occupied by a hint of pearlite. This structural distribution is better illustrated in Fig. 3b, a SEM micrograph magnifying the area at the arrow in Fig. 3a. The center of Fig. 3b features an empty space embedded within the metal matrix consisting mostly of ferrite. Here the ferrite grains appear darker against their bright boundary regions filled with pearlite. The carbon level as inferred from the structure in Fig. 3a and b is therefore not high enough to have a significant effect on material properties. This observation indicates that the parts specified by arrows a and b in object #2 of Fig. 2 were not given any treatments to raise their carbon level.

Figure 3c, an EDS spectrum taken at the arrow in Fig. 3b, demonstrates that the particle specified is a compound consisting of iron and oxygen. It should be noted here that the carbon peak did not stem from the particle but from the thin carbon layer coated on the specimen surface for the SEM analysis. Similar oxide particles are also visible inside the empty space shown in Fig. 3b. These non-metallic inclusions are often observed in slag particles introduced during smelting or subsequent iron making processes. Such peculiar iron oxide particles consistently observed in most specimens under investigation indicate that the raw iron material came from smelting in bloomery furnaces.

The optical micrographs shown in Fig. 3d–3f present structures observed in the specimen taken from the blade at arrow c in object #2. In contrast to that from the blade on the other side of the pick (arrow a), the specimen from this blade displays a visible structural contrast between the internal and external parts, as seen in Fig. 3d. Magnifying the respective areas indicated by arrows 1 and 2, Fig. 3e and f show that the former consists completely of pearlite while the latter contains a substantial fraction of ferrite, demonstrating the contrast that arises from different carbon levels. This non-uniform carbon content is also noted in the variation of Vickers hardness from around 260 to 160 VHN in the external (Fig. 3e) and internal (Fig. 3f) parts, respectively. The decrease in carbon concentration toward the interior as seen in Fig. 3d is an unmistakable sign of a carburization treatment applied to the specific part, the blade marked by arrow c, for raising its carbon level. Object #2 has two blades, of which only one was carburized with no evidence of such a treatment noted for the other.

Objects #3 and 4, axes with a non-symmetric blade and a hole for furnishing a haft, were nearly identical in their microstructural distribution as observed in the respective specimens taken at arrows a, b, and c of either object. It was noted that all the specimens except those from the prominent corners of both axes (arrow b) were made primarily of ferrite, suggesting that the material supplied for their manufacture was derived from low carbon iron. Two exceptional specimens, however, are seen in Fig. 4a, an optical micrograph showing the structure at arrow b of object #3, to consist of high carbon steel, which was quenched to form the martensite phase. The contrast visible in Fig. 4a reflects varying levels of carbon concentration, which are responsible for the decreasing Vickers hardness in Fig. 4a from approximately 600 VHN at arrow 1 to 500 VHN at arrow 2. The effect of this difference in carbon content is also evident in Fig. 4b and c, SEM micrographs magnifying the structure at arrows 1 and 2 of Fig. 4a, respectively, where the difference in the size scale and shape of martensite is significant.

Objects #5 and 6, plate-type axes with a normal symmetric blade, also showed a non-uniform microstructural distribution as determined by carbon concentrations and thermal treatments. In both objects, the specimens from the blade (arrows a and b) were found to have their carbon level greatly increased while those away from the blade (arrows

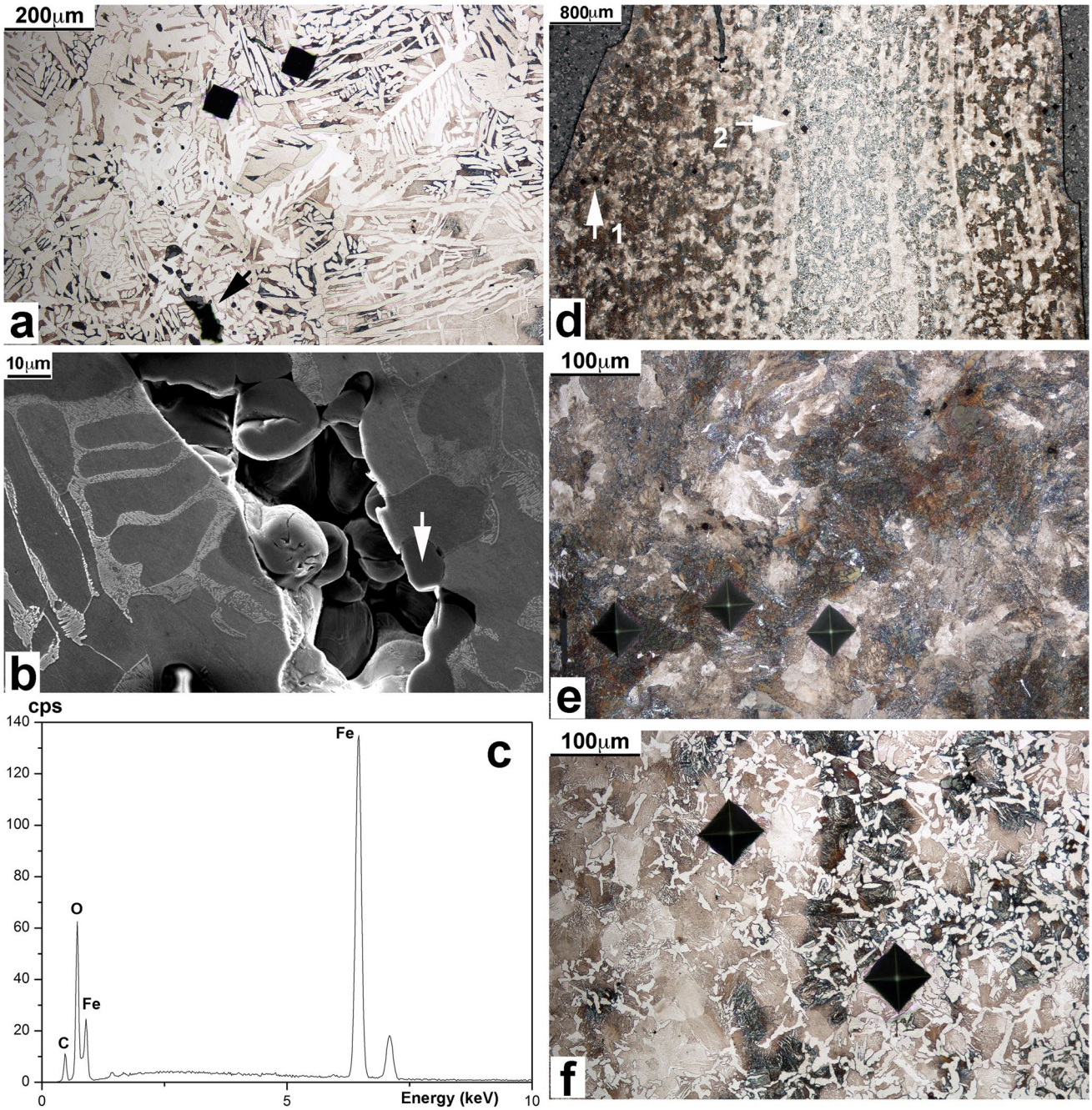

Fig. 3 Micrographs and EDS spectrum. **a** Optical micrograph showing the structure at arrow b of object #2 in Fig. 2, which is composed of rod- or needle-like ferrite grains with their boundaries filled with pearlite; **b** SEM micrograph enlarging the area marked by the arrow in Fig. 3a, where an empty space is located within the metal matrix consisting mostly of dark ferrite grains with their boundaries filled with bright pearlite; **c** EDS spectrum taken at the arrow in Fig. 3b, showing that the particle specified is a compound consisting of iron and oxygen. The presence of such peculiar iron oxide particles is suggestive of bloomery iron employed as a raw material; **d** optical micrograph showing the structure at arrow c of object #2 in Fig. 2. Note the visible structural contrast between the core and external parts; **e**, **f** optical micrographs magnifying the areas indicated by arrows 1 and 2 in Fig. 2d, respectively. Note that the exterior of the given specimen consists exclusively of pearlite while the interior contains substantial ferrite. This structural difference reflects the carbon concentration decreasing toward the interior. The Vickers hardness value as inferred from the size of the indentation marks varies from around 260 in the higher carbon exterior (Fig. 3e) to 160 VHN in the lower carbon interior (Fig. 3f). This decrease in carbon concentration toward the interior is indicative of a carburization treatment applied to the specific part

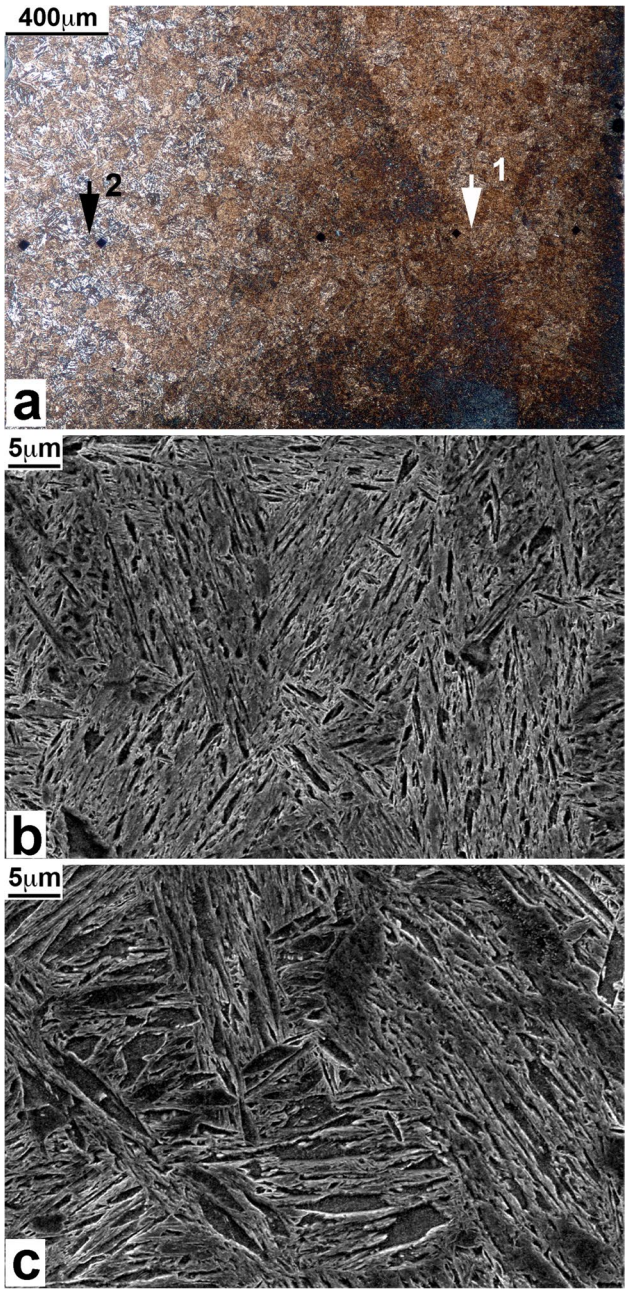

Fig. 4 Micrographs. **a** Optical micrograph showing the structure at arrow b of object #3 in Fig. 2. The micrograph is filled with martensite derived from the quenching of high carbon steel, with the contrast reflecting non-uniform carbon concentration, which is responsible for the decreasing Vickers hardness from approximately 600 VHN at arrow 1 to 500 VHN at arrow 2; **b**, **c** SEM micrographs enlarging the areas marked by arrows 1and 2 in Fig. 4a, respectively. Note the difference in the scale and shape of martensite indicative of varying carbon levels

c and d) were all made of low carbon iron. The blade part of object #5 was made primarily of martensite derived from high carbon steel. In contrast, the specimens from the blade of object #6 were filled with varying proportions of ferrite in the background of extremely fine pearlite. The structure at arrows c and d in both axes consisted of a mixture of ferrite and pearlite.

The specimens from arrows a and b of object #7 were nearly identical and filled with ferrite grains without evidence of any special treatment for raising carbon levels upon completion of the forging to shape. The structure at arrow c of object #8 was also found to consist primarily of ferrite grains. Those at the blade (arrows a and b) of object #8, however, were distinctly different as illustrated in Fig. 5a, an optical micrograph covering the entire cross-section of the specimen taken from arrow b. In this micrograph, martensite is seen to serve as a major constituent, which appears dark against the bright ferrite phase. Note in Fig. 5a that the upper half of the specimen is composed mostly of martensite as opposed to the lower half where bright ferrite grains in the dark martensite background outline the presence of laminated structures.

Figure 5b presents an optical micrograph magnifying the area marked by the arrow in Fig. 5a after a 90° clockwise rotation. The Vickers hardness, as inferred from the size of the indentation marks, is seen to decrease in the right half of the specimen from around 700 to 600 VHN toward the interior. In the left half, however, the hardness alternates between around 300 and 400 VHN, with the lower values measured in the bright ferrite layers. The decrease in hardness in the right half represents a carbon profile decreasing toward the interior, which portrays a reaction occurring during the process of carburization. The alternating layers of high and low carbon materials observed in the left half of Fig. 5b, however, suggest that the material used in that part was prepared separately and then welded to the other half to form the blade of object #8. Another possibility is that a metal piece with a layered structure was carburized only at one side such that the distinction between layers gradually disappeared with the diffusion of carbon atoms from the surface during carburization. If the process had been terminated prematurely, the result would have been the structural distribution as seen in this specimen.

Figure 6a, an optical micrograph, shows the structure of object #9, which is commonly observed in cast iron whose carbon content is less than the eutectic composition, 4.3%. In Fig. 6a, the dark areas in the form of dendrites are covered with pearlite while the bright inter-dendritic areas are filled with cementite. The overall carbon content as inferred from the microstructure is approximately 2.5–3.0%. Figure 6b, an EDS spectrum taken from the area visible in Fig. 6a, reveals the presence of small amounts of silicon (Si), phosphorus (P), and sulfur (S) with their fraction determined at about 0.3, 0.8, and 0.3%, respectively. Here the last two elements were usually derived from iron ores or fuels used in the smelting of cast iron. In contrast, the presence of silicon is indicative of higher smelting temperatures at which silica

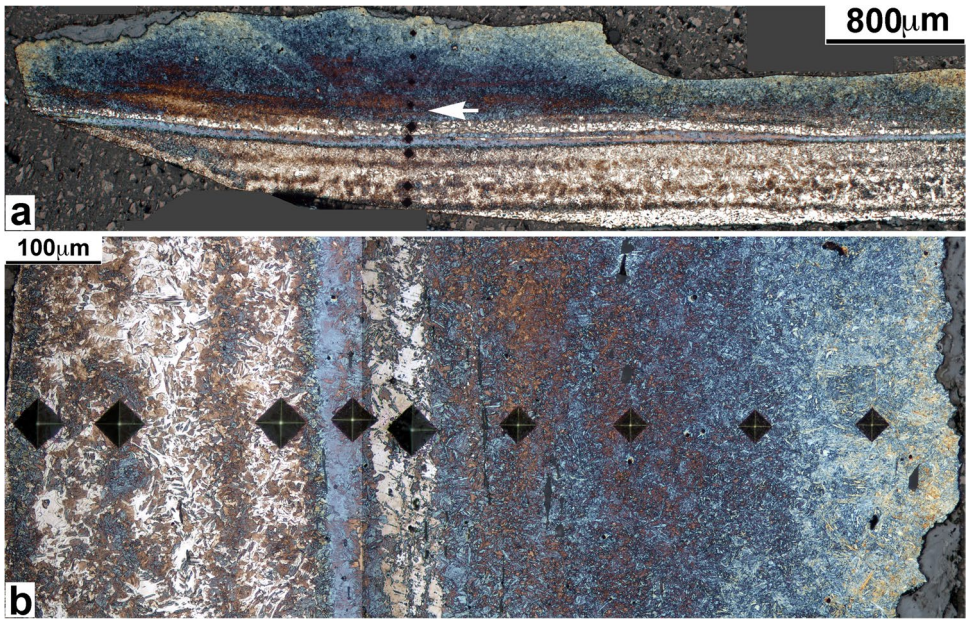

Fig. 5 Optical micrographs. **a** Micrograph covering the entire cross section of the specimen taken at arrow b of object #8 in Fig. 2. The micrograph consists primarily of dark martensite with some ferrite covering the bright areas. Note the upper half filled with martensite as opposed to the lower half showing alternating layers of bright ferrite and dark martensite; **b** micrograph magnifying the area marked by the arrow in Fig. 5a, after a 90° clockwise rotation. In the right half of the micrograph, the Vickers hardness decreases from around 700 to 600 VHN toward the interior while in the left half, the hardness alternates between around 300 VHN in the ferrite-dominated layers and 400 VHN in those filled with martensite. The decreasing hardness in the right half represents a carbon profile decreasing toward the interior, depicting a reaction that occurred during carburization

(SiO_2) can be reduced to elemental silicon to dissolve in iron (Rostoker and Bronson 1990: 107–112).

Discussion

The microstructure data presented above show that, except those from the key functional parts such as the pointed end and the blade edges, all specimens were made of iron materials whose carbon content was not enough to produce any notable effect on material properties. This suggests that iron of negligible carbon content was employed as the primary raw material for making the objects under investigation. The presence of non-metallic inclusions, characteristic of slag from smelting in bloomery furnaces, in the majority of the specimens examined, reveals that this raw material was of bloomery origin. With the exception of object #9 made of cast iron, those in Fig. 2 were all shaped by forging low carbon bloomery iron and then given varying treatments to improve their functional properties.

The high carbon structures found only in the edged blades of objects #2 (a pick), #3–6 (axes), and #8 (an adze) confirm that their carbon levels were raised through a carburization treatment applied to specific parts. This technique for carbon control, which was often implemented together with quenching for further strengthening, demonstrates the level of technological sophistication available at the time. Note that the low carbon iron found in some key functional parts, which generally require high carbon content, should not be understood as a lack of technological experiences. For instance, the use of low carbon iron in object #2 at one of the blades (arrow a) but not at the other (arrow b) was most likely intended as an effort to fulfill two different functional requirements anticipated of the particular tool in service. On the other hand, object #7, made entirely of low carbon iron without raising carbon level even at the blade (arrow a), suggests that it may have been an unfinished product waiting for a further treatment. The technological tradition as observed above may be characterized by 3 traits: (1) bloomery iron produced as a raw material, (2) carburization for carbon control, and (3) proper thermal technique for optimizing functional properties.

Another fact of significance revealed in the microstructure of objects #3 and 4 is the evidence showing that the treatments of carburization and quenching were strictly focused on only one of the asymmetric corner (arrow b for both) of their blade, with the rest of the part given no such special treatments. Despite being identified as axes, the objects in question must have functioned by depending primarily on the prominent corner, which is in strong contrast to normal axes such as objects #5 and 6 of Fig. 2, where their entire blade was hardened by a nearly uniform treatment.

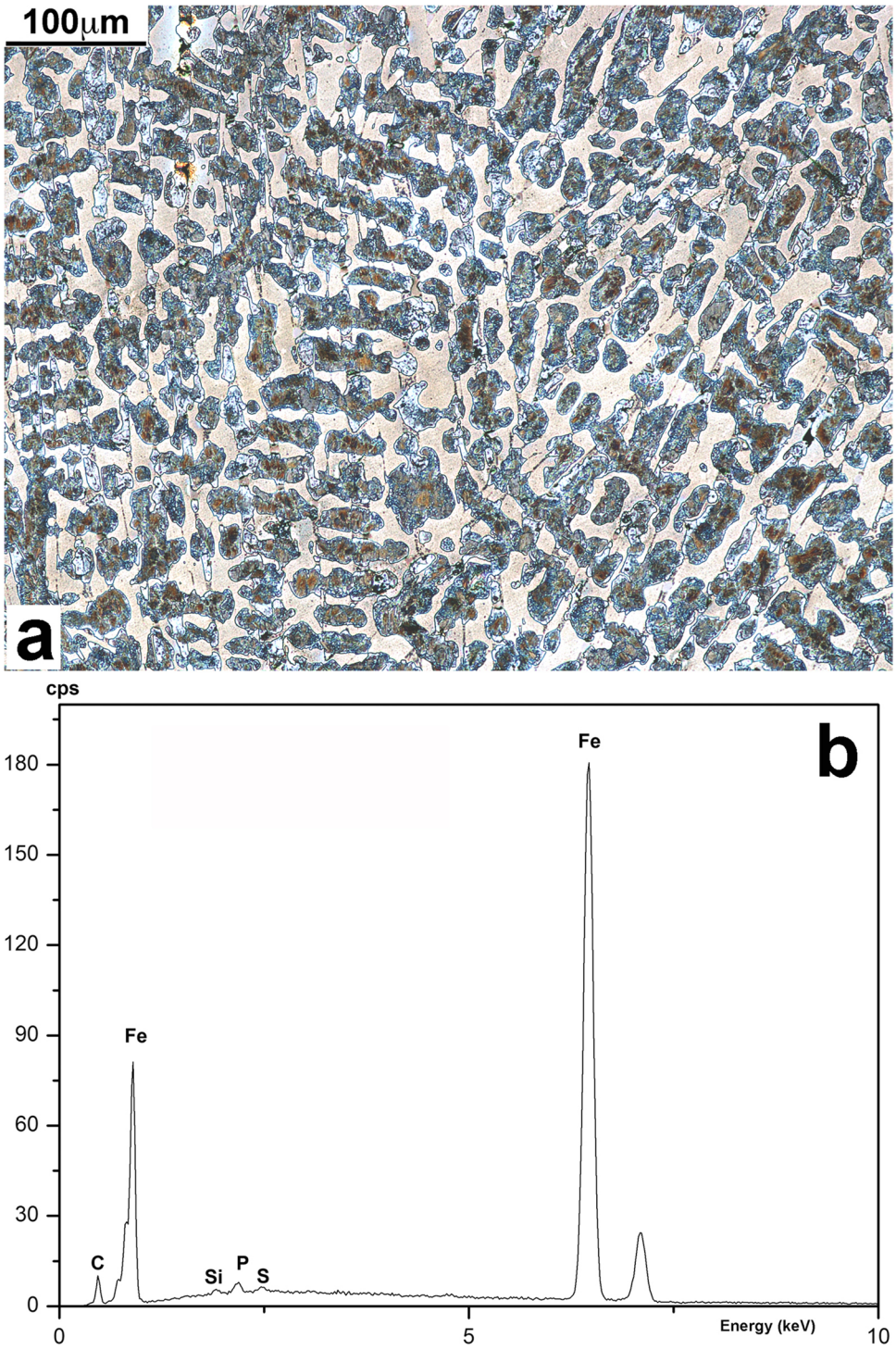

Fig. 6 Micrograph and EDS spectrum. **a** Optical micrograph showing the structure at the arrow of object #9 in Fig. 2. The particular structure is commonly observed in hypoeutectic cast iron whose carbon content is less than 4.3%. The dark dendritic areas represent pearlite while their boundary regions are filled with cementite. The microstructure allows the overall carbon to be determined at approximately 2.5–3.0%; **b** EDS spectrum taken from the area shown in Fig. 6a. Note the presence of small amounts of silicon (Si), phosphorus (P), and sulfur (S) with their fraction determined at about 0.3, 0.8, and 0.3%, respectively. Phosphorus and sulfur are usually derived from iron ores or fuels used in the smelting of cast iron while silicon implies higher smelting temperatures allowing silica (SiO_2) to be reduced to elemental silicon to dissolve in iron (Rostoker and Bronson 1990: 107–112)

The radiocarbon result on a carbon sample directly extracted from object #9, made of cast iron, is significant as it provides convincing evidence for the existence of communities able to implement a fully established iron technology during the period of the mid-fifteenth to early seventeenth century AD. This particular time period of the region has little written or material evidence documented of significant human presence. Together with the metallographic data above, the radiocarbon result may then serve to fill the gap in local history by confirming the existence of significant cultural activities at the time. Note that one of the many cast iron objects excavated from the medieval site at Kastek (arrow 2 in Fig. 1b), approximately 100 km to the southwest of the Talgar site, was also radiocarbon dated to

the post-medieval period of the sixteenth to the eighteenth century AD, indicating a similar cultural activity in progress in the neighboring area (Park and Arnabai forthcoming).

In addition, the ^{14}C concentration of the specific date range constitutes an unmistakable indication of a charcoal-fueled smelting of cast iron. Cast iron objects excavated from Mongolia, however, showed clear evidence of a charcoal-to-mineral coal transition, which likely began during the Khitan period (10^{th} to twelfth century AD) and was evidently carried forward into the Mongol empire that followed to dominate its cast iron industry (Park et al. 2008, 2019; Park 2015). This transition may have been in keeping with a technological development in China where mineral coal-fired iron smelting was in wide practice from the Song Dynasty (960–1279) onward (Wagner 2008: 311–320). Given the region of Talgar was historically under strong influence from both Mongolia and China, object #9, made of charcoal-smelted cast iron long after the beginning of charcoal-to-coal transition in these areas, highlights the possibility of a smaller scale on-site production in practice to fulfill the local demand for cast iron.

Conclusion

A group of nine iron objects recovered from an enclosed space of the medieval site at Talgar in southeast Kazakhstan was subjected to metallographic and radiocarbon analysis. In contrast to most objects excavated thus far from medieval contexts, a carbon sample extracted from the only cast iron object in the given assemblage was radiocarbon dated to the post medieval period of the mid-fifteenth to the early seventeenth century AD. The metallographic data above showed that the particular iron-working tradition reflected in the objects examined may be characterized by (1) production of bloomery iron as a primary raw material; (2) mechanical working for fabrication; (3) carburization applied to the critical parts to raise their carbon concentration; (4) functional properties optimized by the specific quenching technique directed strictly at the critical parts; and (5) limited use of cast iron only as an auxiliary material.

This technological tradition is nearly identical to that reported by Park and Voyakin (2013) on the iron objects excavated at different sectors within the same Talgar site dating approximately to the tenth to thirteenth century AD. A similar iron tradition was also reported for the iron objects recovered from the medieval site at Kastek (arrow 2 in Fig. 1b, Park and Arnabai forthcoming). The iron traditions at Talgar and Kastek consistently employed bloomery iron as a major raw material to be forged into shape. Carburization was consistently practiced as a key method of steelmaking, with the carburized parts being quenched frequently. This study produced evidence of an iron-making tradition that was maintained across the greater Semirechye region including Talgar and Kastek approximately from the seventh century onward. During this time period, charcoal-smelted cast iron was also used continuously, though on a smaller scale and mostly as an auxiliary material for making less important items such as domestic and farming implements.

The unique iron-making tradition above is virtually identical to that which had long been practiced in Mongolia for approximately a millennium from the Xiongnu to the Mongol period as previously mentioned. The only difference was found in the use of mineral coal in Mongolian cast iron production, which apparently began during the Khitan period and came to dominate the following Mongol empire (Park et al. 2008; Park 2015). It should be noted that the bloomery-based iron tradition implemented in the regions of Semirechye and Mongolia was fundamentally different in technological and historical contexts from the cast iron-based tradition that dominated the Chinese iron industry from the Han period (206 BC-220 AD) onward (Rostoker and Bronson 1990; Tylecote 1992). This difference is hardly expected in theories viewing China as the primary source of knowledge for iron production in these non-Chinese areas. Evidently, the emergence of a specific technological tradition in the region was not necessarily dominated by the influence coming from its nearest neighbors.

Acknowledgements This work would not have been possible without the kind support from the late Dr. K. M. Baipakov, who served as the director of the Margulan Institute of Archaeology of the Republic of Kazakhstan. We gratefully remember and acknowledge his encouraging words and advices.

Funding This work was financially supported by the National Research Foundation of Korea (NRF- 2017R1A2B4002082).

References

Bronk Ramsey C (2009) Bayesian analysis of radiocarbon dates. Radiocarbon 51:337–360

Chang C, Tourtellotte PA, Baipakov KM, Grigoriev FP (2002) The evolution of steppe communities from the bronze age through medieval periods in Southeastern Kazakhstan (Zhetysu), The Kazakh-American Talgar Project 1994–2001, Sweet Briar, Almaty Kazakhstan

Donahue DJ, Linick TW, Jull AJT (1990) Isotope-ratio and background corrections for accelerator mass spectrometry radiocarbon measurements. Radiocarbon 32(2):135–142

Frachetti MD (2008) Pastoralist landscapes and social interaction in Bronze Age Eurasia. University of California Press, Berkeley Los Angesles and London

Frye RN (2004) The heritage of Central Asia. Markus Wiener Publishers, Princeton

Larreina-Garcia D, Li Y, Liu Y, Martinón-Torres M (2018) Bloomery iron smelting in the Daye County (Hubei): technological traditions in Qing China. Archaeological Research in Asia 16:148–165

Park JS (2015) The implication of varying ^{14}C concentrations in carbon samples extracted from Mongolian iron objects of the Mongol period. J Archaeol Sci 63:59–64

Park JS, Arnabai N (forthcoming) The implication of technological diversity reflected in the iron assemblage from the medieval site in southeast Kazakhstan

Park JS, Chunag A, Gelegdorj E (2008) A technological transition in Mongolia evident in microstructure, chemical composition and radiocarbon age of cast iron artifacts. J Archaeol Sci 35:2465–2470

Park JS, Eregzen G, Yeruul-Erdene Ch (2010) Technological traditions inferred from iron artefacts of the Xiongnu Empire in Mongolia. J Archaeol Sci 37:2689–2697

Park JS, Honeychurch W, Chunag A (2019) The technological and chronological implication of ^{14}C concentrations in carbon samples extracted from Mongolian cast iron artifacts. Radiocarbon 61(3):831–843

Park JS, Reichert S (2015) Technological tradition of the Mongol Empire as inferred from bloomery and cast iron objects excavated in Karakorum. J Archaeol Sci 53:49–60

Park JS, Voyakin D (2009) The key role of zinc and tin in copper-base objects from medieval Talgar in Kazakhstan. J Archaeol Sci 36(3):622–628

Park JS, Voyakin D (2013) Characterization of iron technology at medieval Talgar in Kazakhstan. In: Rehren Th, Humphris J (eds) The World of Iron. Archetype Publications, London, pp 234–242

Reimer PJ et al (2020) The IntCal20 Northern Hemisphere radiocarbon age calibration curve (0–55 cal kBP). Radiocarbon 62(4):725–757. https://doi.org/10.1017/RDC.2020.41

Rostoker W, Bronson B (1990) Pre-industrial iron its technology and ethnology. Archaeomaterials Monographs No.1, Philadelphia, Pennsylvania

Tylecote RF (1992) A History of Metallurgy. The Institute of Materials, London

Wagner DB (2008) Science and Civilization in China, Volume 5, Part 11: Ferrous Metallurgy. Cambridge University Press, Cambridge